Indian Journal of Pure & Applied Physics
Vol. 61, August 2023, pp. 645-652
DOI: 10.56042/ijpap.v61i8.326

Non-aqueous Solution Processed CdZnTe Thin Film via Chemical Bath Deposition: Effect of Zn doping Variation

Sudeshna Surabhi[a]*, Kumar Anurag[b] & S R Kumar[b]

[a]Brindavan College of Engineering, Yelahanka, Bengaluru, Karnataka, 560 063, India

[b]Thin Film Laboratory, National Institute of Advanced Manufacturing Technology, Ranchi 834 003, India

Received 18 April 2023; accepted 14 July 2023

In recent years, compounds from the chalcogenide family have gained importance in thin film technology due to their potential applications in photovoltaic cells, X-ray and gamma-ray detectors. CdZnTe is a II–VI compound semiconductor and is used in photovoltaic solar cells due to its high efficiency and tunable band gap. CdZnTe thin films have properties intermediate between those of CdTe and ZnTe. Their addition creates a common lattice in which the energy band gap is larger than that of ZnTe, making the material more attractive for electronic device fabrication. In this work, CdZnTe films (X = 0.1M, X= 0.2M, and X=0.5M) were deposited on a nickel substrate by chemical bath deposition in a non-aqueous medium. The growth parameters of the CdZnTe film can be adjusted by varying the concentration (X=0.1M, X=0.2M, and X=0.5M) of the Zn content. The varying Zn content regulates the growth rate of CdTe and is an important factor affecting the properties of the film. The chemical bath deposition method was used to vary the different Zn concentrations in the range of 0.1M, 0.2M, and 0.5M, and their effects on various properties of the CdZnTe films were investigated. The effects of Zn doping on the structural, morphological, elemental, and optical properties were studied by XRD, SEM, EDS, FTIR, UV-Visible, and PL. The X-ray diffraction study showed that all films have a cubic zinc-blende structure with a (111) plane. The crystallite size was calculated using the Scherrer formula, and it was found that the crystallite size decreases with increasing Zn content.

Keywords: Cadmium Telluride; Cadmium Zinc Telluride; Thin Films; Optical Properties; X-ray Diffraction; Crystal Structure; Preferential Orientation

1 Introduction

Recently II-VI metal chalcogenide[1] and alloys have received considerable attention from researchers due to the significant progress in the deposition technique as well as their wide applications in the optoelectronic devices used in the UV-Visible and near IR regions of the electromagnetic spectrum. These II-VI semiconductor materials are highly appealing due to their impressive physical properties. One noteworthy characteristic is their tunable optical properties, which can be effectively controlled by adjusting factors such as mole fraction, particle size, and morphology. Over the past few years, there has been notable advancement in the field of semiconductor-based nuclear radiation detectors. These detectors now find extensive use across various domains such as nuclear physics, X-ray and gamma-ray astronomy, and nuclear medicine. The imaging capabilities, excellent energy resolution, and compact system fabrication make them highly appealing when compared to other detectors like gas detectors and scintillators. Traditional semiconductors such as silicon (Si) and germanium (Ge) have been widely utilized in radiation detectors due to their impressive performance across various applications[2]. The field of applications has seen significant growth, which has spurred the development of detectors based on compound semiconductors[2,3]. Compound semi-conductors have an advantage in that they can be grown with a wide range of physical properties (such as band gap, density, and atomic number). Making them suitable for almost any application. There has been particular interest in radiation detectors that operate at room temperature leading to the development of compound semiconductors with wide band gaps composed of silicon and germanium. Furthermore, compound semiconductors with high atomic numbers have been favored for detecting X-rays and gamma rays as they enhance photoelectric interaction. Typically, compound semiconductors are derived from elements found in the III and V groups (*e.g.*,

*Corresponding author:
(E-mail: surabhisudeshna@gmail.com)

GaAs) and the II and VI groups (*e.g.*, CdTe) of the periodic table. In addition to binary compounds, ternary materials like CdZnTe have also been prepared. Cadmium zinc telluride (CdZnTe) is a compound semiconductor that shows great promise as a radiation detector. It offers several advantages, such as good energy resolution, high detection efficiency, and the ability to operate at room temperature. Additionally, CdZnTe thin films possess properties that fall between those of CdTe and ZnTe. This combination results in a common lattice with a larger energy band gap than CdTe making CdZnTe even more attractive for the fabrication of electronic devices. The compound semiconductor CdZnTe is characterized as a direct band gap semiconductor, with a band gap that ranges from 1.5 to 2.4 eV at room temperature[4]. To control the growth parameters of the CdZnTe film, one can adjust the concentration of Zn content. The presence of different levels of Zn content helps regulate the growth rate of CdTe and has a significant impact on the properties exhibited by the film. CdZnTe thin films show higher resistivity, typically in the range of 10^{10} Ωcm, and high resistivity is particularly important for the development of CdZnTe-based detectors because this property makes it possible to use these detectors at room temperature without the need for cryogenic cooling. Besides these properties, CdZnTe exploitation in solid-state applications is still limited by some important problems. The low mobility- lifetime product of carriers(especially holes) hinders the use of thick detectors[5]. Another main issue to be solved is the realization of durable contacts with good adhesion and reproducibility.

In this work, we investigate the growth of CdZnTe thin films prepared by chemical bath deposition in a non-aqueous medium with different Zn concentrations (X=0.1M, 0.2M, and 0.5M) and the effect of Zn doping on the structural, morphological, and optical properties was carried out.

2 Experimental Procedure

CdZnTe films were chemically deposited on a nickel substrate with dimensions of 1.5 x 1 cm^2. The substrate (nickel) was cleaned in a soap solution and then rinsed with distilled water. The substrate was then cleaned with acetone in an ultrasonic bath for 10 minutes, rinsed with distilled water, and finally air dried. The electrolyte was prepared using 0.05M TeO_2, 0.05M cadmium acetate, 0.125M sodium borohydrate, and $ZnCl_2$(X) dissolved in 40ml ethylene glycol. The temperature of the non-aqueous bath was maintained at 160 °C. Then, the nickel substrate was immersed in the electrolyte using a rigid holder. The electrolyte was aged for four hours. The electrolyte was stirred moderately and deposited for 15 minutes. Different Zn concentrations [X=$ZnCl_2$] ranging from 0.1 to 0.5 M were varied in this procedure. After deposition, the substrate was removed from the electrolyte and washed with distilled water. The structural features of the deposited CdZnTe thin films with different Zn concentrations were measured using a high-resolution Rigaku Miniflex model 600 diffractometer with CuKα radiation (wavelength λ = 1.5418Å). Surface morphology and elemental analysis of the films were performed using a scanning electron microscope and EDS (Jeol JSM390LV) at an electron beam energy of 10 KeV. The optical properties of the films were measured using a fluorescence spectrophotometer (RF–5301PC, Shimadzu) at a wavelength of 200 to 800 nm.

3 Results and Discussion

3.1 Structural Analysis

XRD spectra of as-grown CdZnTe thin films with varying Zn concentration (X = 0.1M, X= 0.2M, and X=0.5M) are shown in Fig. 1, and the inset graph shows the XRD spectra of as-deposited CdTe thin film. The as-deposited CdZnTe film with varying concentrations of Zn (X = 0.1M, X= 0.2M, and X=0.5M) are deposited on the Ni substrate. The films are physically stable and show good adhesion. The XRD spectra are sustained in the 20-80° span with a scan rate of 3°/min. From the figure, we observe that all the as-deposited concentration change Zn doped CdZnTe films exhibit peaks attributed to (111) plane with reflection at 2θ = 23.01° and show that the films have cubic zinc blende structure. Its intensity increases with increasing zinc concentration in the films. All the varying Zn concentration CdZnTe films have the same characteristics and show the same preferential orientation. XRD spectra give the information that the concentration change CdZnTe (X = 0.1M, X= 0.2M, and X=0.5M) as grown films have cubic zinc blende structure exhibits peaks corresponding to (111), (220), (311), (222), (400), (331), (420) and (422) planes with reflection at 2θ = 23.01°, 40.41°, 45.86°, 51.22°, 56.87°, 62.77°, 67.64° and 71.21° respectively. Reflection of Cd and CdTe are also observed at 2θ = 38.23° and 27.72° with (101) and (200) planes, respectively, which is also observed in as-deposited

CdTe thin film as observed from the inset graph. Reflection of CdTe observed due to phase inclusion. The preferred planes and observed 'd' values of varying Zn concentrations of as-deposited CdZnTe films are shown in Table 1. The average crystallite size of pure CdTe, as well as doped CdTe with varying Zn concentrations, were calculated using the Scherrer formula:

$$D=\frac{0.9\lambda}{\beta cos\theta} \quad \ldots (1)$$

Where β is the full width at half maxima (FWHM) in radian, λ is the x-ray wavelength (0.154nm), and θ is the angle of diffraction[6–8]. It indicates that films are nanopcrystalline. It is observed that the crystallite size (D) decreases with increasing Zn concentration[7] because the width of the diffraction peak increases due to the increase in lattice microstrain, and we see a decrement in crystallite size shown in Table 2. It indicates that the dopant ion (Zn^{2+}) replaced the Cd^{2+} in the parent CdTe matrices. The microstrain (ε) developed in varying Zn content films was calculated by using the following relation(Eqn.,2)[8] and is shown in Table 2. Fig. 2(a-b) depicts the variation of FWHM(β) and crystallite size and FWHM(β) and microstrain(ε) as a function of Zn doping concentration.

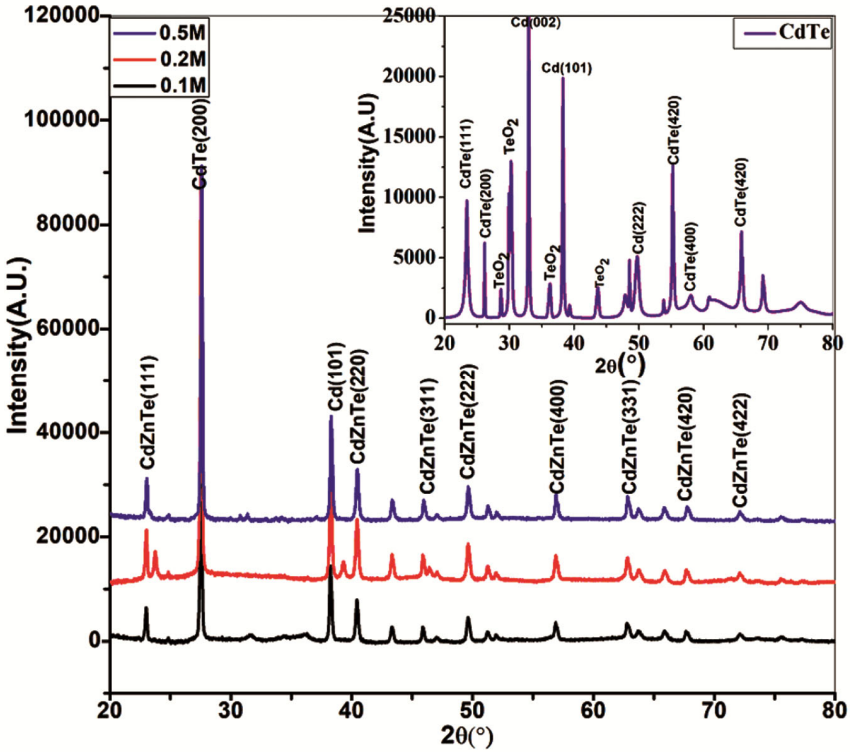

Fig. 1 — XRD spectra of as deposited CdZnTe thin films with varying Zn concentration & inset graph showing XRD spectra of as cast CdTe thin films

Table 1 — 2θ, 'd', FWHM and Miller-Indices of as deposited CdZnTe thin films with varying Zn concentration

Zn Concentration(X=0.1, 0.2 and 0.5) CdZnTe as deposited						Standard Values		Miller Indices
X=0.1		X=0.2		X= 0.5				
2θ	d(Å)	2θ	d(Å)	2θ	d(Å)	2θ	d(Å)	
23.72	3.75	23.01	3.86	23.00	3.86	23.75	3.74	(111)
40.42	2.23	40.42	2.23	40.45	2.23	41.01	2.20	(220)
45.87	1.98	46.43	1.95	45.87	1.96	46.87	1.94	(311)
51.23	1.78	51.24	1.78	51.27	1.78	50.50	1.81	(222)
56.87	1.62	56.87	1.61	56.90	1.62	56.83	1.62	(400)
62.77	1.48	62.78	1.48	62.77	1.45	62.47	1.49	(331)
67.65	1.38	67.66	1.38	67.70	1.38	66.83	1.40	(420)
72.08	1.31	71.22	1.32	71.29	1.33	71.29	1.32	(422)

$$\varepsilon = \frac{\beta \cos\theta}{4} \quad \ldots (2)$$

3.2 Surface Morphology and Elemental Compositional Study

Figure 3 (a-d) shows the SEM images and Fig. 3 (e-h) Shows particle size distribution histogram of pure and doped CdTe thin films with varying Zn concentration (X = 0.1M, X= 0.2M, and X=0.5M). It can be seen that the morphology of the nanocrystals did not show much changes following Zn^{2+} doping. The micrograph reveals a compact surface with grains interconnected to each other. From the figure, it is also observed that the films are uniform, grains are distinct and coaxial. No evidence of cracking was observed in the films, even after prolonged storage. The grains' distribution is very much dependent on the concentration of Zn. However, particle size increases with increasing concentration of Zn in the host CdTe matrices, and some sort of cluster formation is observed[9]. The average particle size was calculated using Gaussian fitting to the size distribution histogram and was obtained as 0.389, 1.420, 1.490 and 1.96 μm respectively, for pure CdTe and doped CdTe with varying Zn concentration. The grains are unevenly distributed over the surface with a zinc concentration of 0.1M. This may be due to the formation of colloidal particle in the solution[9]. At 0.1M the nickel surface is not uniformly active, and the adsorption occurs at specific preferential sites only where isolated hemispherical tellurium nuclei can be seen. CdZnTe film with 0.2M Zn concentration exhibits surfaces with equal size grains distributed all over the surface in cluster forms. At 0.5M Zn concentration, it is clear that isolated hemispherical

Table 2 — Structural parameters of as deposited CdZnTe thin films of varying Zn concentration

S. No.	Varying Zn Concentration	FWHM (degree)	Crystallite size (nm)	Micro Strain ($\times 10^{-4}$)
1.	Pure CdTe	0.345	24.6	14.73
2.	$CdZn_{X=0.1M}Te$	0.120	68	5.11
3.	$CdZn_{X=0.2M}Te$	0.162	50.29	6.91
4.	$CdZn_{X=0.5M}Te$	0.252	32.2	12.19

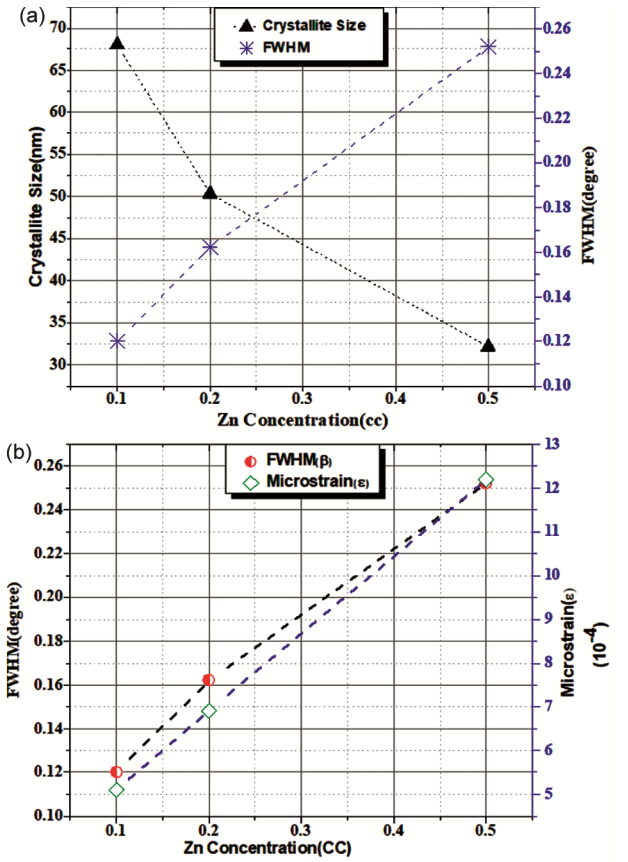

Fig. 2 — (a)Variation of FWHM(β) and Crystallite size(D) as a function of Zn doping variation & (b) Variation of FWHM(β) and microstrain(ε) as a function of Zn doping.

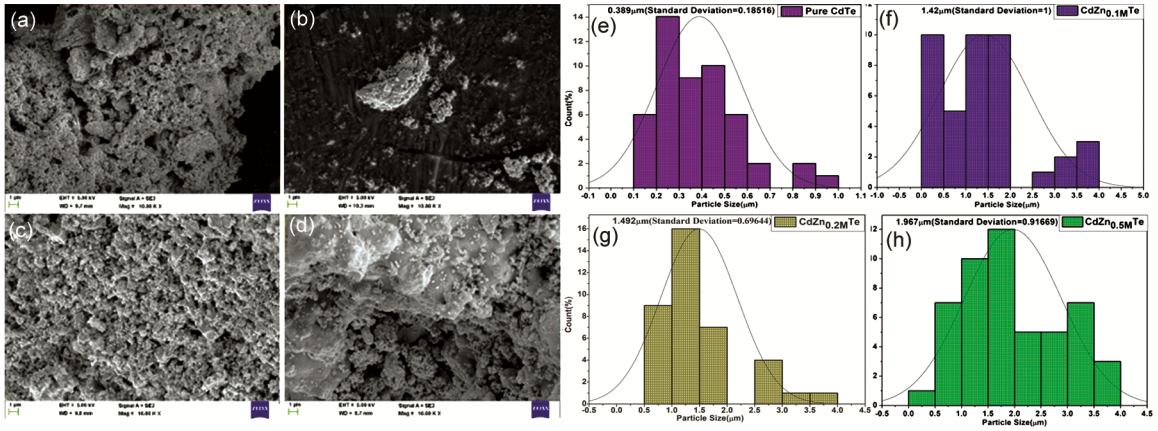

Fig. 3 — (a-d) SEM image of pure and doped CdTe thin films with varying Zn concentration and (e-h) corresponding particle size distribution histogram determined from SEM images.

nuclei grow and coalesce to form bigger clusters, and no cloudy surface is observed, as shown in Fig. 3(d).

The elemental analysis of pure and Zn-doped CdTe with varying Zn concentration are performed with the help of energy dispersive spectroscopy (EDS). The EDS spectra were recorded in the binding energy of 0-20 KeV. The EDS spectra of pure CdTe and Zn-doped CdTe with varying Zn concentrations are shown in Fig. 4(a-d). From the spectra, the peaks of Cd, Zn, and Te make an appearance in all the cases, which are distinct and clearly seen. However, some traces of oxygen are also seen, but it is not mentioned in the spectra. The presence of oxygen is due to surface contamination. The atomic percentage of Cd, Zn, and Te of pure and doped samples are given in Table 3. From the table, we observe that as the concentration of Zn increases, the ratio of the atomic percentage of Cd and Te is nearly equal to 1 in the highest concentration of Zn-doped CdTe thin films that indicates films have stoichiometric nature, which is suitable for device application. Notably, the elemental analysis results are consistent with the dopant concentration employed to prepare the samples.

3.3 FTIR Analysis

Figure 5 shows the FTIR transmission spectrum of the as-deposited pure and doped CdTe thin films with varying Zn concentration (X = 0.1, X= 0.2, and X=0.5) over the wave number ranging from 400 – 4000 cm^{-1}. The FTIR spectra give the idea of quality and impurities present in the deposited thin films. The FTIR spectra revealed that the IR transmittance and absorption intensity were found to increase with the increase in Zn concentration. This is because at higher concentration, lattice misfits like

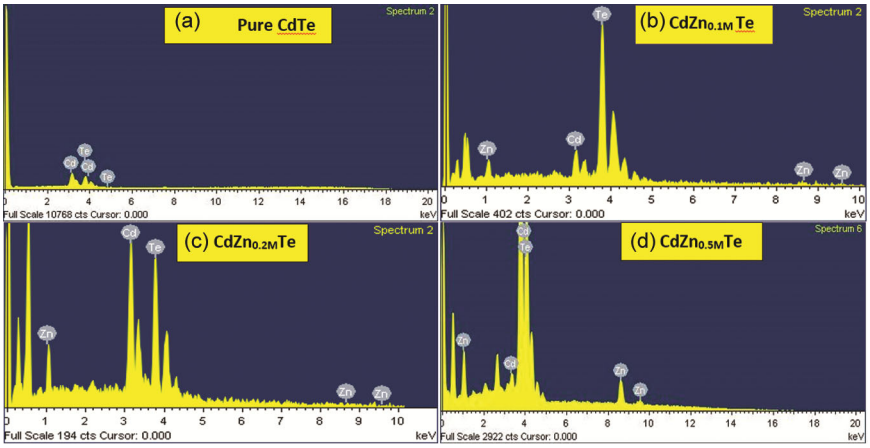

Fig. 4 — (a-d) EDS Spectra of pure CdTe and Zn doped CdTe with varying Zn concentration.

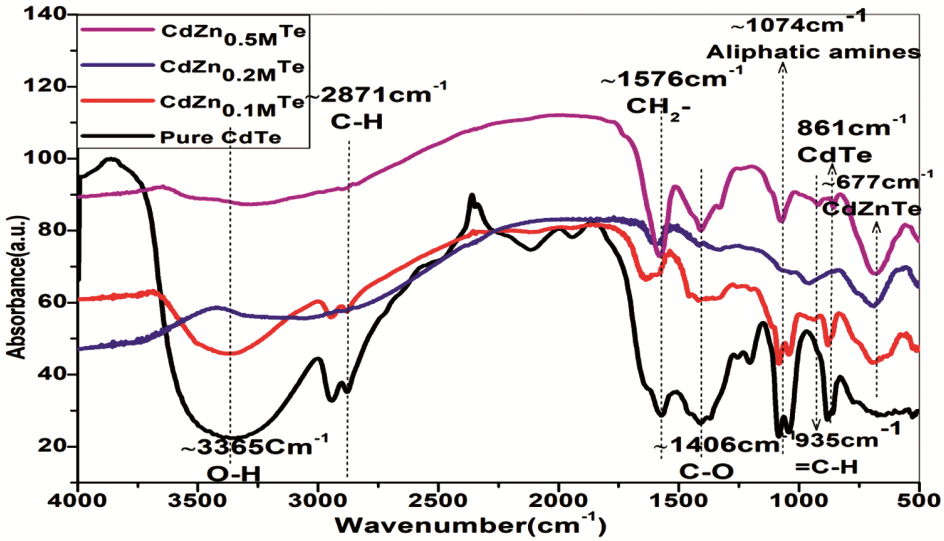

Fig. 5 — FTIR Spectra of pure and doped CdTe thin films with varying Zn Concentration.

dislocations and micro-precipitates decrease and are responsible for higher IR lattice absorption. From the figure, we observe that both pure and doped CdTe shows the IR spectra of alkenes (=C-H), aliphatic amines, C-O,CH_2-, CH and OH. The IR spectra of CdZnTe occur at ~677cm^{-1} in the case of doped CdTe[10]. However, the peak of CdTe occurs at 861cm^{-1} in the case of pure CdTe. C-O functional group occurs due to ethylene glycol. The broad peak at ~3408 cm^{-1} indicates the existence of OH functional groups, which originates the cause of the atmosphere[11].

Table 3 — Atomic percentage of Cd, Zn and Te of pure and doped CdTe film with varying Zn concentration

S. No.	Elements	Atomic %			
		X= 0.00 M	X = 0.1 M	X = 0.2 M	X = 0.5 M
1	Cd	52.59	37.05	37.75	46.68
2	Zn	0.00	0.00	5.12	10.07
3	Te	47.05	52.18	53.32	57.83

Table 4 — Different functional groups appeared in pure and doped CdTe film with varying concentration

S. No	Functional Groups	Wavenumbers (cm^{-1})
1.	CdZnTe	~677
2.	CdTe	~861
3.	=C-H	~935
4.	Aliphatic amines	~1074
5.	C-O	~1406
6.	CH_2-	~1576
6.	C-H	~2871
7.	O-H	~3408

Different functional groups and their corresponding wavenumber that appeared in pure and doped CdTe thin films are given in Table 4.

3.4 Thermoluminescent Properties

3.4.1 UV-Visible analysis

UV-Visible spectroscopy is an effective tool for monitoring the optical properties of thin films. The absorption spectra of Pure & doped CdTe film with varying Zn concentrations (X=0.1,0.2 & 0.5) were studied at room temperature in the wavelength span of 250-800nm. CdZnTe is a direct band gap semiconductor and therefore, its band gap is determined by Tauc's relation[12,13] *i.e.*

$$(\alpha h\vartheta)^2=A(h\vartheta-E_g)^{1/2} \quad \ldots (3)$$

where α is the absorption coefficient, h is Planck's constant, ϑ is the vibration frequency, A is the proportionality constant, and Eg is the band gap. From this relation, we plot a graph of photon energy(hϑ) vs $(\alpha h\vartheta)^2$, and the extrapolation of the curve i.e.$(\alpha h\vartheta)^2=0$, gives the energy band gap of the film[7]. Fig. 6 shows the curve of photon energy Vs $(\alpha h\vartheta)^2$ of pure and doped CdTe films with varying Zn concentrations. The absorption spectra confirm that due to variation in Zn concentration, the absorption edge shift towards a shorter wavelength. At 0.5M as deposited CdZnTe film cover a larger area of shorter wavelength as compared to other concentration, and this happens due to structural change in the film which increase the grain size. It is also observed that

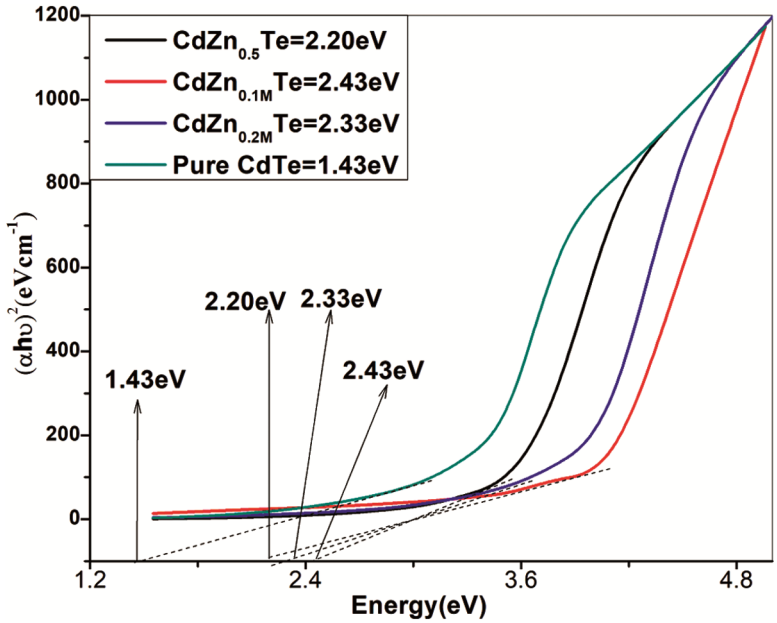

Fig. 6 — Band gap of $CdZn_XTe$(X=0.0M, 0.1M, 0.2M and 0.5M) nanocrystalline films.

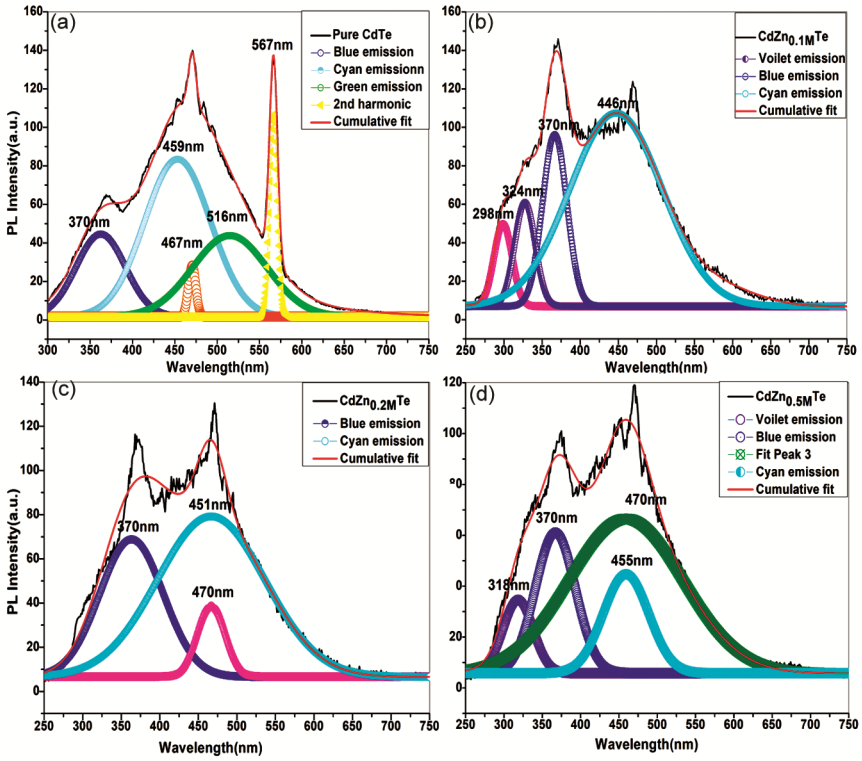

Fig. 7 — PL Spectra of (a) Pure CdTe (b) $CdZn_{X=0.1M}Te$ (c) $CdZn_{X=0.2M}Te$ (d) $CdZn_{X=0.5M}Te$ nanocrystalline thin films.

the energy band gap (E_g) for each Zn concentration is different. The band gap variation of different Zn concentrations is linear because the band gap of CdTe is smaller than ZnTe. When the Zn concentration changes from X= 0.1M to 0.5M, the band gap of the films varied in the range from 2.43, 2.33 and 2.20eV. The decrement happens due to the formation of solid solution with varying Zn concentration[9]. Another reason is that as the Zn concentration increases, there is a chance of the formation of a secondary phase that leads to a decrease in the band gap. The third possible reason is that Zn^{2+} ions replace Cd^{2+} ions in the CdTe lattice. However, band gap (E_g) of pure CdTe nanocrystalline film is estimated to be 1.43 eV lower than bulk CdTe(1.56 eV). Hence the absorption edges of the as-obtained pure CdTe nanocrystals have obviously redshift. The crystallite size of all the nanocrystalline film in this experiment is beyond the exciton Bohr radius of CdTe(15.0nm)[14]. The change in Eg values might be replaced of Cd sites by the Zn(dopant) in the host CdTe lattices.

3.4.2 Photoluminescence Studies

Photoluminescence studies are carried out using a spectrophotometer with a wavelength ranging from 200 to 800 nm on excitation with a wavelength of 270nm. Fig. 7(a-d) shows the PL spectra of pure and doped CdTe with varying Zn concentrations. Since the measurement was taken up without the use of filters, the presence of second harmonics at 567 nm is inevitable and can be seen as line spectra along with the PL peaks in the case of pure CdTe.(Fig. 7(a)). All the PL samples show blue emission at 370 nm due to excitation at higher energy level emission and recombination of excitation or trapped hole pair[9]. Instead of blue emission, pure CdTe also exhibit green emission at ~516 nm due to excitonic luminescence and intra-band transitions, *i.e.*, between levels created by defects within the band gap caused by the oxygen vacancies[15,16]. The variation in concentration results in the sharp increase in emission intensity at ~370 nm, along with the appearance of a new peak in the visible region. The cyan emission has been appeared in all PL samples due to inter-grain boundary defects. However, the peak at ~470 nm is influenced by the transition from band minimum to band maximum *i.e.*, their band gap. With the addition of Zn to CdTe nanocrystals, the PL emissions of the nanocrystalline films blue shift to a shorter wavelength side, and the PL emission intensity is significantly increased with increasing concentration of dopant ions.

4 Conclusions

Our studies have clearly demonstrated the advantages of an ethylene glycol-based bath for chemical bath deposition of pure and different concentrations of Zn-doped CdTe nanocrystalline films on a Ni substrate. The high solubility of the cadmium and tellurium sources and the high operating temperatures enable us to deposit stoichiometric CdZnTe films. XRD confirms that the films produced exhibit a cubic phase. All the films show the same properties as well as the same preferred orientation, and it was observed that the crystallite size decreases with increasing Zn content in the films, which is an expected result since the ionic radius of Zn is smaller (0.74Å) than that of Cd (0.97Å), and this causes increased intercalation of Zn^{2+} ions in Cd^{2+} sites. The morphology of the pure and doped CdTe films shows a crystalline and narrow distribution of nearly spherical particles, with the average particle size increasing with increasing Zn content. Below 0.5M, the grains are unevenly distributed over the surface due to the formation of colloidal particles in the solution. At 0.5M, a spherical structure appears over the entire surface of the film. EDX analysis revealed that the composition of the various elements in the films is consistent with the amount of dopant added during fabrication. The optical energy band gap of pure CdTe was found to be redshifted compared to the bulk of CdTe. The band gap of Zn-doped CdTe films was also redshifted with increasing dopant concentration. However, with the addition of Zn to CdTe nanocrystals, the PL emission of the nanocrystalline films shifts to shorter wavelengths, and the PL emission intensity increases significantly with increasing dopant ion concentration. Moreover, further increase in Zn concentration leads to poor crystalline structure and morphological disorder. Moreover, the thermoluminescence properties of these thin films can provide useful information about the surface states, which could explain the size dependence of the surface fluorescence.

Acknowledgments

The authors are grateful to Director, NIAMT, Hatia, Ranchi for providing necessary research facilities and constant encouragement for this work. Authors are also thankful to CIF BIT, Mesra for all types of characterizations.

References

1 Narayana S T N & Pushpalatha H L, *J Chem Bio Phys Sci Sec C*, 7 (2017) 1119.
2 McGregor D S, Hermon H, *Nucl Instrum Methods Phys Res Sect Accel Spectrometers Detect Assoc Equip*, 395 (1997) 101.
3 Owens A & Peacock A, *Nucl Instrum Methods Phys Res Sect Accel Spectrometers Detect Assoc Equip*, 531 (2004) 18.
4 Jain S, Photoluminescence study of cadmium zinc telluride, West Virginia University, 2001.
5 Schlesinger T E, Toney J E, Yoon H, et al., *Mater Sci Eng R Rep*, 32 (2001) 103.
6 Chander S, Dhaka M S, *Phys E Low-Dimens Syst Nanostructures,* 84 (2016) 112.
7 Anbarasi M, Nagarethinam V S & Balu A R, *Mater Sci-Pol,* 32 (2014) 652.
8 Surabhi S, Anurag K & KumarS R, *Chalcogenide Lett*, 19 (2022) 143.
9 Kumar S, Rajpal S, Sharma S, Roy D & Kumar S R, *Dig J Nanomater Biostruct*, 12 (2017) 339.
10 Chander S & Dhaka M S, *Thin Solid Films*, 625 (2017) 131.
11 Tang H, Yan M, Zhang H, Xia M & Yang D, *Mater Lett*, 59 (2005) 1024.
12 Zha G, Zhou H, Gao J, Wang T & Jie W, *Vacuum*, 86 (2011) 242.
13 Rajashree C, Balu A & Nagarethinam V, *Int J Chem Tech Res*, 6 (2014) 347.
14 Rajh T, Micic O I & Nozik A J, *The J Phys Chem*, 97 (1993) 11999.
15 Chaure S, Chaure N B & Pandey R K, *Phys E Low-Dimens Syst Nanostructures*, 28 (2005) 439.
16 Cross R B M, Souza M M D & Sankara N E M, *Nanotechnology*, 16 (2005) 2188.